EXELFS as a tool for quantifying phase distributions in materials

D. Haskel[†] ,M. Sarikaya[‡] ,M. Qian[‡] ,E. A. Stern[†]

[†] *Department of Physics FM-15*

[‡] *Materials Science and Engineering Department*

University of Washington, Seattle WA 98195 ,USA

(August 11, 1995)

Abstract

A method has been developed to quantify phase distributions in multiphase materials by using the information contained in the EXtended Energy Loss Fine Structure (EXELFS) of a probe atom in an Electron Energy Loss Spectroscopy (EELS) spectrum. The EELS and EXELFS determine, in addition to the atomic composition, the near neighbor atomic environment about each atom type separately. The method is applicable to electron transparent foils observed in a Transmission Electron Microscope (TEM) equipped with a parallel detection electron energy loss spectrometer. The relative amounts of phases that have a common element can be determined even in the presence of additional phases which do not share that common element. The method is particularly applicable to layered materials and can be used, for example, to determine the local relative thickness of a metal and its oxide layer. The Mg/MgO system was used to demonstrate the method, and it was found that the accuracy in relative thickness determination is about 5%. The near edge fine structure information was consistent with the results of the EXELFS analysis.

I. INTRODUCTION

The Extended Energy Loss Fine Structure (EXELFS), i.e., the fine structure superimposed on the high energy loss side of an edge in the EELS spectrum, contains quantitative information about the local structure around the scattering atom from which the core electron is excited. This includes neighboring atom distances, their types and numbers, and structural disorder about equilibrium bond distances, similar to that present in the X-ray absorption fine structure (XAFS) technique [1–3]. By extracting this information one can learn about properties of the system under study which are otherwise inaccessible from the standard analysis of the EELS spectrum.

Much of the literature that exists on applications of EXELFS analysis is aimed at determining local structure around a given atom type in single-phase materials [4–8]. However, being able to analyze the EXELFS signal in multiple-phase systems as well, can lead to important quantitative information on both the composition and spatial distribution of the constitutive phases. As an example, consider a system consisting of a pure metal, its oxide layer and a third, oxygenated, phase which does not contain the metallic atom and whose structure is unknown. Finding the relative amounts of the pure metal and its oxide from standard atomic compositional analysis will be extremely difficult, since the EELS signal at the oxygen edge includes contributions from both the oxide and the oxygenated phase, whose structure is unknown. However, since the EXELFS signal of the metallic atom contains information on the local structure around that atom, it will include contributions from both the metallic and oxide phases but not from the third phase. By analyzing this signal, one can obtain the relative amounts (and therefore thickness in a layered system) of the two phase components, irrespective of the presence of the third phase.

There are a number of techniques to determine the local thickness of a specimen in the TEM. Some of these are: (i) convergent beam electron diffraction, applicable only for a relatively thick region of the sample (i.e., $t \gg \xi$, where ξ= extinction distance) and for a crystalline material; (ii) intensity of the plasmon loss relative to that of the zero loss peak in an EELS spectrum, applicable to both crystalline and amorphous single phase materials; (iii) stereomicroscopy in the conventional TEM, not applicable for overlaping thin films and (iv) simulation of the high resolution images, also only applicable to thin ($t < 100$ Å) crystalline materials. The methods (i), (iii) and (iv) are applicable only to single phase crystalline regions without the overlap of a second phase.

The method described in this paper can measure the relative amounts of phases even in overlapping thin films with different compositions and crystallinity using the EXELFS signal, provided that the phases have at least one common element (the probe atom). Relative thickness determination in this way, particularly for amorphous structures, has never been possible before, especially for ultra-thin overlapping layers. Even in the absence of long range order, the EXELFS signal contains information on the short range order in the amorphous phase which usually allows one to determine the first nearest neighbor configuration around the excited atom. Diffraction and imaging techniques require that the phases be crystalline.

Another distinct advantage of this method is that it can exploit the full capabilities of the TEM, in particular, its very high spatial resolution. By varying the electron probe size or by looking at adjacent parts of the sample one can study spatial inhomogeneities in phase composition (or in relative thickness in a layered system) down to length scales as small as the electron probe size. This could be used, for example, to study roughness of an oxide layer grown on a thin ($\approx 100 - 1000$ Å) metal or semiconductor substrate. The spatial resolution possible presently is $\approx 0.1 \mu m$, and could be reduced to ≈ 100 Å if improvements that reduce radiation damage to the sample and sample drift are made. In addition, the EXELFS information can be supplemented by the information from the other powerful analytic capabilities of the TEM such as imaging and diffraction. In fact, in the case presented here the phases present were identified by diffraction, and the EXELFS determined their relative amounts.

To illustrate the method, the present work shows how information on the local relative thickness of a metal and its oxide layer can be obtained in a system containing Mg, MgO and some organic contamination. In Section II the experimental results are presented. Section

III includes the analysis of the results and discussion and the conclusions are in Section IV.

II. EXPERIMENTAL PROCEDURES

A commercial 99.999 % pure magnesium foil was prepared for the TEM by electropolishing in a 20 % nitric acid 80 % methyl alcohol solution at 2 volts, washed in methanol and dried [9]. The sample was kept in a desiccator for three days and measured. Fig. 1 shows the EELS spectrum containing both oxygen and magnesium K-edges taken in image mode at 200 KV operating voltage and using a 3 mm entrance aperture on the GATAN 666 parallel detector spectrometer. Fig. 2 shows the EELS spectrum containing the C and O K-edges. Fig. 3 displays the selected area diffraction pattern from the same region taken with a nominal camera length L=500 mm. The EELS data of the Mg K-edge shown in Fig. 4 was taken in diffraction mode using a nominal camera length of 250 mm and the same entrance aperture. The presence of an oxygen signal (in Fig. 2) suggests that the sample was oxidized. This assumption is verified by analyzing the selected area diffraction pattern as discussed below. Low loss spectra as well as diffraction patterns were taken before and after irradiation to monitor any structural change or thickness variation due to radiation damage to the sample. No detectable change was observed in any of the above mentioned. The average thickness of the region studied is $t = 0.25\,\lambda_{\rm e}$ as calculated from the zero loss - plasmon peak spectra (λ_e is the average electron mean free path for inelastic scattering in this sample). As shown in Fig. 2, a carbon signal was also detected in the low-loss region of the EELS spectrum. The reason for a carbon signal appearing in the spectrum is less clear, and may be due to contamination of the surface by some organics left from the polishing process.

One of the questions is whether some of the oxygen on the surface of the sample is bound to carbons in the contamination layer or not. We show that this does not affect the quantitative analysis by using the EXELFS data of Mg regarding the question of the ratio of metal/oxide composition and that we are able to separate the oxygen atoms bound to the magnesium from those bound to the carbon, if any.

III. ANALYSIS AND DISCUSSION

The analysis of the ring pattern shown in Fig. 3 indicates that it corresponds to a sodium chloride structure with a lattice parameter of $a = 4.21$Å, corresponding to that of MgO at room temperature. The average camera length obtained from plotting r, ring radius, as a function of λ/d (λ is the electron wavelength and d is the interplanar spacing) is L=494(7) mm as compared to the nominal camera length of 500 mm with which the pattern was taken. The underlying spot pattern corresponds to the Mg (hcp) structure. If one wants to determine the relative content of the Mg and MgO phases, one cannot use standard compositional analysis since the O signal in the EELS might have contributions from the presence of an organic compound, as already discussed. In this case, however, one can make use of the fine structure on the Mg K-edge as discussed below. Fig. 5 shows the EELS of the Mg K-edge after the pre-edge background was subtracted by fitting to a power law model [10]. Plural scattering was removed from the spectrum by using a standard deconvolution procedure described by Egerton [11]. The post edge background was removed by fitting a cubic spline to the post edge such as to minimize the low frequency components ($R \leq 1\mathring{A}$) of the Fourier transformed EXELFS, $\tilde{\chi}(R)$, with respect to a standard [12]. Fig. 6 shows the EXELFS $\chi(k)$ obtained this way after normalizing by the edge step (k is the excited core electron wavenumber). Fig. 7 shows the amplitude of the complex Fourier transform of $k^2\chi(k)$ using $\chi(k)$ data between 2.5 and 8.5 Å^{-1} (solid lines).

FEFF5, a computer code which calculates the theoretical X-ray Absorption Fine Structure (XAFS) in the dipole approximation [13], was used twice to separately generate the theoretical $\chi(k)$ in Mg and MgO with Mg being the absorbing atom. This calculation is valid for the EXELFS as well, as long as the scattering process satisfies the dipole approximation [14,15]. This is obtained by a proper choice of the collection aperture on the GATAN spectrometer [16].

The fitting of the data to the theory was done in r-space between 1.6 and 3.0 Å which includes the first two shells for the hcp structure of Mg and the first two shells for the MgO structure. (Note that Fig. 7 has its peaks shifted from the actual atom-atom distances because of phase shifts introduced by final state electron-atom interactions [1], but these are accounted for in the analysis.) The k range used for the fitting is that between 2.5 and 8.5 Å^{-1}. The number of parameters allowed in the fit must be less than the number of independent points in the spectra;

$$N = \frac{2\Delta k \Delta r}{\pi} + 2 \tag{1}$$

where Δk and Δr are the k and r ranges used for the fitting [17]. For our case at hand, $\Delta r = 1.4$ Å and $\Delta k = 6$ Å^{-1}, giving $N = 7$. The fitting was done by allowing the following 5 parameters in the theory to vary: (i) The relative weight of the Mg and MgO signal was allowed to vary by weighting the Mg signal amplitude by $(1-y)$ and the MgO signal amplitude by y, so that $(1-y)/y$ is the ratio of Mg atoms in the metallic environment to that of Mg atoms in the oxide environment; (ii) The Debye-Waller factors for the first neighbors distances σ_i^2 (mean square displacements about equilibrium bond length); (iii) A shift to the energy origin of the excited electron from the value found in the theory, ΔE_0, different for each structure. This is because the theoretical value found by FEFF usually differs from the experimental one by a few eV due to (a) the poor estimation in the theory of the interstitial charge density on which the energy reference depends and (b) the experimental value depending on where on the edge step the core excitation energy threshold has been allocated for isolating the EXELFS signal. The passive electrons amplitude reduction factor S_0^2, a many-body correction which accounts for the relaxation of the atomic electrons wave functions in the excited atom to the core hole potential [18], is set to 0.95 and equal for both structures as it depends only on the central atom. The nearest neighbor distances R_i and their coordination numbers N_i were fixed at the values from the known structures (sodium chloride and hexagonal close-packed structures for MgO and Mg respectively).

As mentioned above, the EXELFS data were obtained after subtracting the post edge background and normalizing by the edge step. The edge step normalization causes amplitude distortions in the data which can be corrected by means of a McMaster correction [19]. McMaster corrections are available for X-ray absorption data and special care should be taken when using those corrections in EXELFS data. The energy dependence of the EELS background differs significantly from that of the XAFS if the maximum transverse momentum transfered to the core electron, q_m, is much less than (ω/v), where $\hbar\omega$ is the electron energy loss and v is the speed of the incident electrons [16]. The value of the maximum momentum transfered to the core electron is determined by both the camera length and the entrance aperture to the GATAN spectrometer, since the Mg K-edge data was taken with the microscope in the diffraction mode. The value thus obtained is $q_m \approx 1.5\,\text{Å}^{-1}$, while $(\omega/v) \approx 1\,\text{Å}^{-1}$ at the Mg K-edge energy. In this case, then, the additional energy dependence of the EELS background compared to the XAFS one is logarithmic in nature [20] and the use of a McMaster correction is a good approximation to correctly account for the amplitude distortions in the EXELFS introduced by the edge step normalization.

The dotted line in Fig. 7 shows the results of the fitting using this procedure. The values found for the parameters are the following: y=0.28(4), $\Delta E_{0,Mg}$=4.2(6) eV, $\Delta E_{0,MgO}$=3.4(7) eV, $\sigma^2_{Mg} = 0.016(3)\,\text{Å}^2$, $\sigma^2_{MgO} = 0.003(1)\,\text{Å}^2$. (Note that by allowing a change in the overall ΔE_0 for each structure, chemical effects affecting the energy threshold, specially in the ionic phase, are accounted for [21]).

The value for y indicates that 28% of the probe atoms (Mg) are in the oxide form while 72% are in the metallic form. The Debye-Waller factors obtained for the Mg lattice are consistent with the known value for the Debye temperature of magnesium, estimated from the correlated Debye model [22] as follows. In this model, in the high temperature limit, $T \geq \Theta_D/2$, one has

$$\sigma^2 = \frac{K_B \cdot T}{M_r \cdot \omega_E^2} \tag{2}$$

where M_r is the reduced mass of the bond, ω_E is the Einstein frequency of the bond, K_B is Boltzmann constant, Θ_D is the Debye temperature, and T is the temperature. For first shell bonds, it can be shown that [22]

$$\omega_E \approx \frac{3}{4}\omega_D \tag{3}$$

where ω_D is the Debye frequency. Since $\hbar\omega_D = K_B\Theta_D$, $\Theta_{D,Mg}$ =318K [23] and T=300K, substituting into Eq. 2 gives $\sigma^2 = 0.02$ Å^2 comparable to the value found in the fitting. For the MgO lattice the same procedure is not applicable since optical phonons dominate the vibrational spectrum and then characteristic Einstein frequencies are significantly different for different bonds. The Debye Waller factors found for the Mg-O bond corresponds to an Einstein temperature of $\Theta_E \approx 900K$ indicating a very strong force constant for this bond. As a comparison, the characteristic temperature for the Cu(1)-O(4) apical bond in the superconducting $YBa_2Cu_3O_7$ is $\Theta_E \approx 800K$ [24].

From the value of y obtained by the EXELFS analysis we can calculate the relative thicknesses of the metal and the oxide by noting that

$$\frac{n_{(Mg,MgO)} \cdot t_{(MgO)}}{n_{(Mg,Mg)} \cdot t_{(Mg)}} = \frac{y}{(1-y)} = 0.39(6), \tag{4}$$

($n_{x,z}$ is the number of atoms of type x per unit volume of phase z and t_x is the thickness of phase x) and then, accounting for the different values of the volume per Mg atom in the metal and its oxide, to obtain,

$$\frac{t_{(MgO)}}{t_{(Mg)}} = 0.32(5) \tag{5}$$

Fig. 8 compares the Mg K-edge spectra obtained in this experiment with that obtained in pure MgO [25]. The MgO data has a characteristic sharp line on top of its white line corresponding to a transition of the excited electron to a bound state, whose character can be verified, e.g., by comparing to a theoretical calculation of the band structure of the solid (density of states). Regardless of its origin, this sharp feature causes the “shoulder” observed in the combined spectrum taken with a poorer resolution compared to the pure MgO spectrum. This feature can then be used as the energy reference to align the two spectra.

The edge step is proportional to the number of Mg atoms in the measured region of the sample. From the EXELFS analysis we found the relative amounts of Mg atoms in the two different environments. By normalizing the two signals to their respective edge steps, we can subtract from the combined spectrum the appropriate amount of MgO signal ($\approx 28\%$) and this way the pure Mg loss spectrum can be obtained.

We want to emphasize that this procedure is valid only semiquantitatively because the spectra were taken with different energy resolution. The spectrum so obtained is compared with the pure magnesium results reported by Zaluzec [26] in which plural scattering contributions were not removed from the spectra. For comparison, then, for this particular procedure, plural scattering was not removed from our spectrum either, though it is expected to be a small effect since the samples were very thin ($\mathrm{t} \leq 0.3\,\lambda_\mathrm{e}$).

Fig. 9 shows the resulting spectra after subtracting different percentages of MgO signal. As mentioned before, the result is mostly reliable above the edge where the energy dependence of the spectrum is smoother and small differences in energy resolution between the two spectra have less impact. The results thus obtained are in reasonable agreement with the pure Mg data reported by Zaluzec [26,27] when one subtracts $\approx 25\%$ of the MgO signal, in agreement with the results obtained from the EXELFS.

After determining the relative amount of the metallic and oxide phases, the question still remains whether the oxygen is only bound to magnesium in the oxide phase or also to the carbons in a third phase as well. To answer this question, we first use standard EELS compositional analysis to find the ratio of atomic oxygen to that of atomic magnesium (by using the spectra in Fig. 1). We found that ratio to be $[O]/[Mg]$ =0.35(5). The uncertainties in the standard analysis can be estimated by using different energy ranges for pre-edge background removal as well as for intensity integration. For this procedure, K-edges were measured since the $\mathrm{L}_{2,3}$ edges of Mg are at an energy loss $\Delta E \approx 51$ eV, a region where the standard power-law background removal method is not very accurate [28]. Since the O and Mg K-edges are separated by $\Delta E \approx 800$ eV in the loss spectrum, one can measure them on the same spectrum using a resolution of 1 eV/channel, without the need of splicing different measurements into a common energy scale, a procedure which might introduce additional errors in the compositional analysis. It may be noted that, since the spectra shown in Fig. 1 were taken in the image mode, the result of the compositional analysis might be subjected to a small amount of error. This is due to the fact that, in the image mode, electrons of different energy losses are accepted from an area somewhat larger than that defined by the entrance aperture to the spectrometer. In the present case, however, this error which originates from chromatic aberration is not significant, because the oxide layer, presumably, uniformly covers the metal on both surfaces.

If the oxygen content of the sample were to be *only* in the MgO phase, we can calculate the oxygen to magnesium atomic ratio expected, since the relative thickness of Mg and MgO are known. As found from the EXELFS the relative thicknesses are given by

$$t_{(MgO)} = 0.32 \cdot t_{(Mg)} \tag{6}$$

and the following holds:

$$\frac{[O]}{[Mg]} = \frac{\frac{4}{Vcell_{(MgO)}} \cdot t_{(MgO)}}{\frac{2}{Vcell_{(Mg)}} \cdot t_{(Mg)} + \frac{4}{Vcell_{(MgO)}} \cdot t_{(MgO)}} = \frac{1}{1 + \frac{Vcell_{(MgO)} \cdot t_{(Mg)}}{2 \cdot Vcell_{(Mg)} \cdot t_{(MgO)}}} \tag{7}$$

(MgO has a sodium chloride structure with four Mg and four O atoms in the unit cell and Mg has the hcp structure with 2 atoms in the unit cell). Substituting in Eq. 7 the respective volumes of the unit cells and using Eq. 6, one obtains a ratio $[O]/[Mg]$ =0.28(5), the uncertainty being estimated from the uncertainty in the thickness relation. The results of the EXELFS and of the standard compositional analysis are then consistent with a model in which the oxygens are bound to only the magnesium atoms in the MgO phase and not to the carbons. We now compare the near edge fine structure of the O K-edge in the mixed sample to that in pure MgO [25], as shown in Fig. 10. The O K-edge spectrum of MgO was measured at T=110K while the present experiment was done at room temperature. The effect of different temperatures on the spectrum is larger at higher energy losses from the edge because the Debye-Waller-like factor in the XAFS equation decreases with increasing excited core electron wavenumber [18]. The slight differences in the two spectra can then be attributed to thermal disorder and different energy resolution. The result of the compositional analysis and the similar ELNES signals obtained for the O K-edge compared to that in pure MgO suggests that the oxygen atoms are mainly bound to magnesium atoms in the MgO phase and not to the carbon atoms in a third phase. If the oxygen were present in an organic contamination layer it is likely that oxygen mass loss would occur rapidly at the doses used to record the EXELFS data, an effect which was not observed.

IV. CONCLUSIONS

We showed that important information regarding phase composition can be obtained in a multiple-phase system by extracting the information contained in the EXELFS signal of a given atomic species. In this way, the relative thickness of a metal and its oxide layer was found in a very thin film. This allowed a separation of the spectrum for the pure metal when the spectrum of the pure oxide is known. This information combined with standard elemental compositional analysis was used to deduce the environment of the O atoms, indicating that most were bound as MgO and not to the carbon contamination, consistent with the near edge fine structure analysis of the O K-edge. The information given by the EXELFS analysis complements and adds to the powerful analytic capability of the TEM. In this case, selected area diffraction detected the presence of and identified the two phases containing the Mg atoms but could not determine their relative amounts. It should be noted that the analysis used in this paper was not dependent on the phases being in a layered configuration. Any topological distribution of the two phases would have been amenable to the same analysis, e.g., if the phases were MgO particles embedded in the metal.

The main limitation of this method lies in the amount of information available in the fine structure (see Eq. 1), which restricts the number of variables allowed in fitting. This is especially important for the EXELFS of low-Z elements, since their rapidly decaying background limits the k range usable for the analysis.

This approach is a powerful new method for investigating multiple phase-systems where the structure of some of the phases is unknown and phase compositional analysis is still desired. In particular, thin materials with overlay-film geometry, such as semiconductor/native-oxide systems, are just one of a variety of systems where this method can prove very important in the plan-view orientation (such systems can be observed in the traditional way by HREM in cross-sectional samples, but this is difficult for thin (≈ 500 Å) samples). Moreover, for mixtures of phases with lower dimension than planar, such as quantum dots or wires, the technique here is still applicable. The high spatial resolution attainable in the TEM can be exploited to study spatial inhomogeneities in phase composition on length scales as small as the electron probe size.

REFERENCES

[1] D. E. Sayers, E. A. Stern and F. W. Lytle, Phys. Rev. Lett **27**, 1204 (1971).

[2] R. D. Leapman and V. E. Cosslett, J. Phys. D **9**, L.29-32 (1976).

[3] D. E. Johnson, S. Csillag and E. A. Stern, Scanning Electron Microsc. **1** 105 (1981).

[4] B. M. Kincaid, A. E. Meixner and P. M. Platzman, Phys. Rev. Lett. **40**, 1296 (1978).

[5] A. E. Kaloyeros, R. B. Rizk and J. B. Woodhouse, Phys. Rev. B **38**, 13099 (1988).

[6] V. Serin, G. Zanchi and J. Se'vely, Microsc. Microanal. Microstruct. **3**, 201-212 (1992).

[7] K. Hssein, G. Zanchi, J. Sevely, X. Devaux, A. Rousset, EMAG -MICRO 89, London, 13-15 September 1989.

[8] M. Qian, M. Sarikaya, and E. A. Stern, in Proceedings of the 51st Annual Meeting of the Microscopy Society of America, (San Francisco Press, San Francisco, 1993) pp. 578-579.

[9] J. W. Edington, in "Practical Electron Microscopy in Material Science", (Van Nostrand Reihhold).

[10] R. G. Egerton, Electron Energy Loss Spectroscopy in the Electron Microscope, (Plenum Press, New York , 1986) pp. 255-262.

[11] R. G. Egerton, Electron Energy Loss Spectroscopy in the Electron Microscope, (Plenum Press, New York , 1986) pp. 247-254.

[12] M. Newville, P. Livins, Y. Yacoby, J. J. Rehr, and E. A. Stern, Phys. Rev. B **47**, 14126 (1993).

[13] J. J. Rehr, J. Mustre de Leon, S. I. Zabinsky, R. C. Albers, J. Am. Chem. Soc. **113**,

5135 (1991).

[14] M. De Crescenzi, CRC Critical Reviews in Solid State and Materials Sciences, **15**, Issue 3 (1989).

[15] R. D. Leapman, P. Rez ,D. F. Mayers, J. Chem. Phys. **72**(2), 1232 (1980).

[16] E. A. Stern, M. Qian, M. Sarikaya, "Spatially resolved local atomic structure from EXELFS". Proceedings of the Material Research Society, vol.332, M. Sarikaya, K. Wickramasinghe and M. Isaacson (eds.) (MRS, Pittsburgh, 1994) pp. 1-12.

[17] E. A. Stern, Phys. Rev. B **48**, 9825 (1993).

[18] E. A. Stern and S. Heald in *Handbook on Synchrotron Radiation*, Vol. 1, ch.10, edited by E. E. Koch. North-Holland, 1983.

[19] W. H. McMaster *et al. Compilation of X-ray Cross Sections* Lawrence Radiation Laboratory Report UCRL-50174 (National Bureau of Standards, Springfield VA, 1969).

[20] E. A. Stern, Optik **61**,No 1, 45 (1982).

[21] P. A. Lee and G. Beni , Phys. Rev. B **15**, 2862 (1977).

[22] E. Sevillano, H. Meuth and J. J. Rehr, Phys. Rev. B **20**,4908 (1979).

[23] N. Ashcroft and N. Mermin, in *Solid State Physics* (international edition, edited by D.Garbose.Crane), p. 461.

[24] D. Haskel and E. A. Stern, to be published.

[25] M. Qian, unpublished data

[26] J. Zaluzec , Ultramicroscopy **9**, 319 (1982)

[27] R. G. Egerton, Electron Energy Loss Spectroscopy in the Electron Microscope, (Plenum Press, New York, 1986) p.206 .

[28] D. R. Liu and D. B. Williams, Proc. Roy. Soc. Lond. **A425**, pp.91-111 (1989).

FIGURES

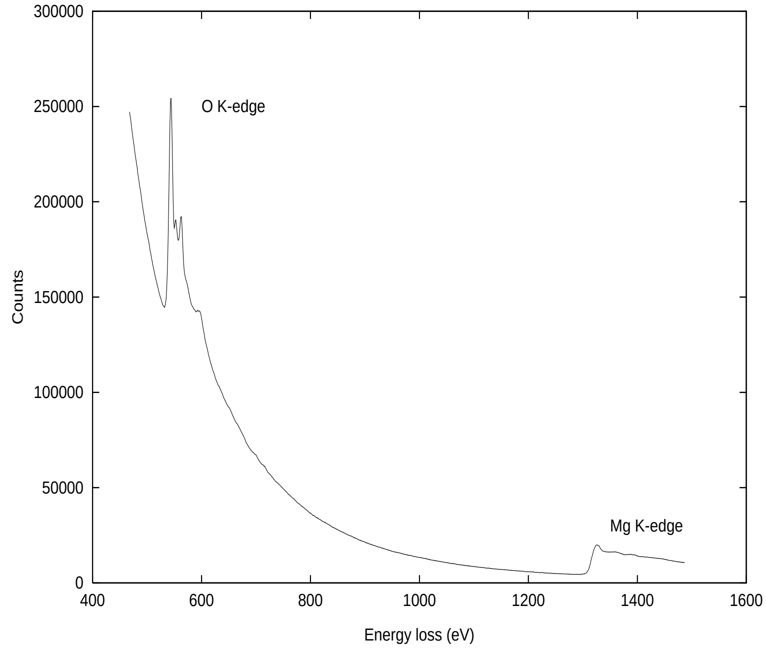

FIG. 1. O and Mg K-edge EELS spectrum taken in image mode at 200 KV operating voltage and using a 3 mm entrance aperture to the GATAN 666 parallel detection spectrometer.

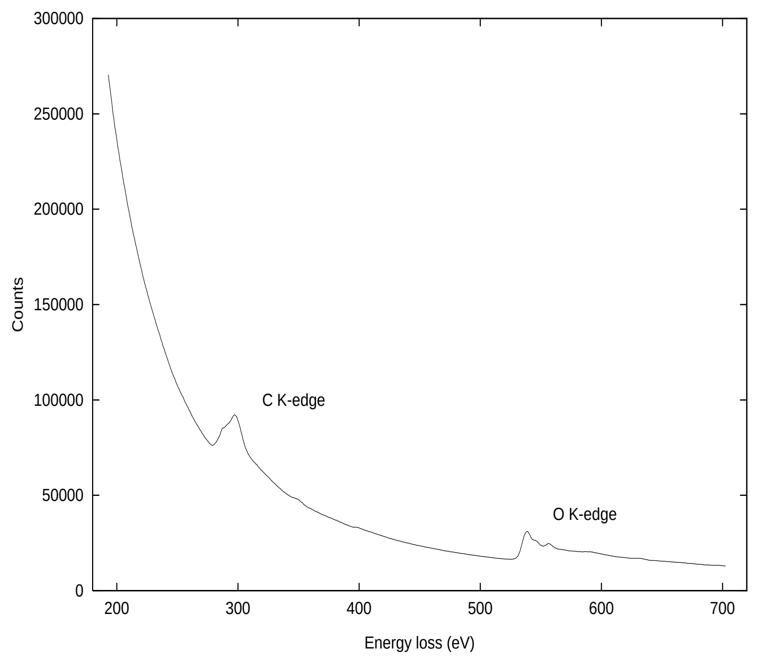

FIG. 2. EELS spectrum with C-and O K-edges taken in the image mode at 200 KV operating voltage and a 3 mm entrance aperture.

FIG. 3. Selected area diffraction pattern of the area studied using a nominal camera length of L = 500 mm.

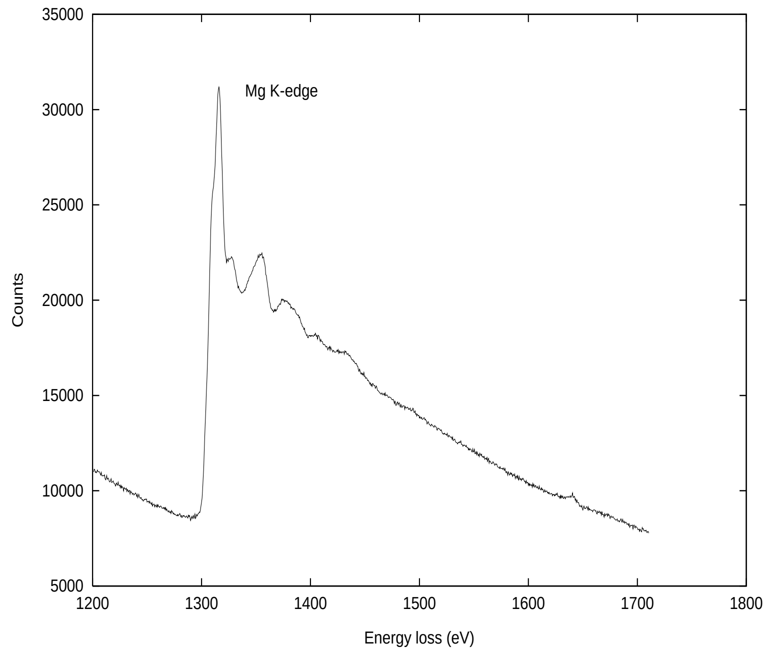

FIG. 4. EELS spectrum displaying Mg K-edge taken in the diffraction mode using a nominal camera length L = 250 mm and a 3 mm entrance aperture.

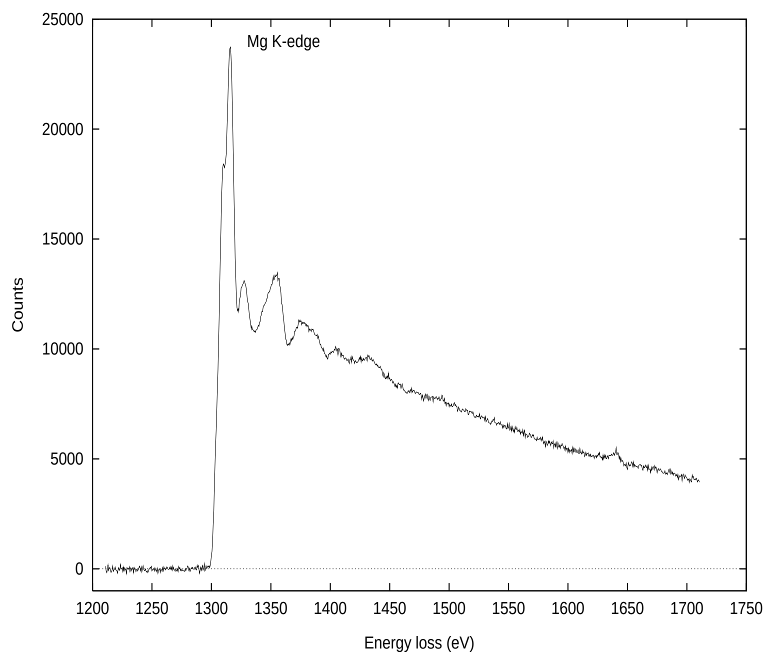

FIG. 5. Mg K-edge EELS data after removal of the pre-edge background and plural scattering.

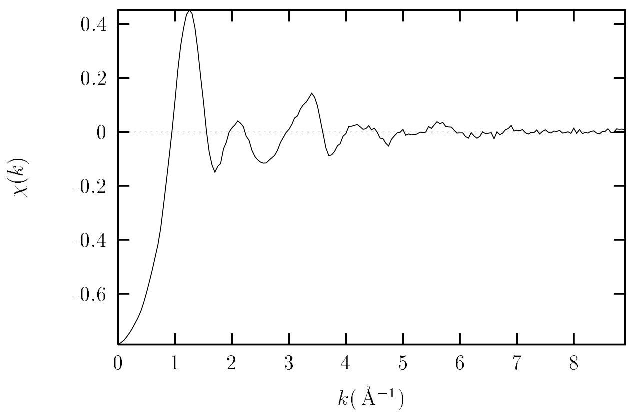

FIG. 6. EXELFS data $\chi(k)$ obtained for the Mg K-edge after post-edge background removal and normalization by the edge step.

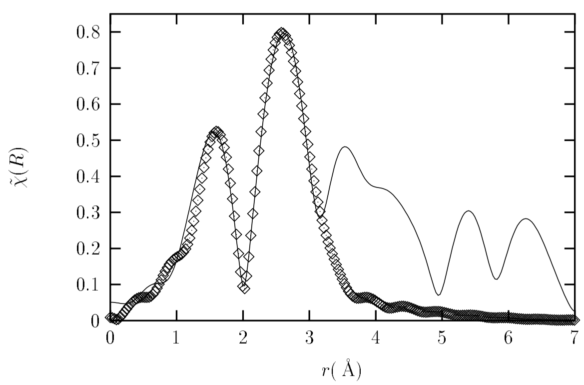

FIG. 7. Amplitude of the complex Fourier transform of the Mg K-edge EXELFS. Solid line is the experimental data and the points are theory.

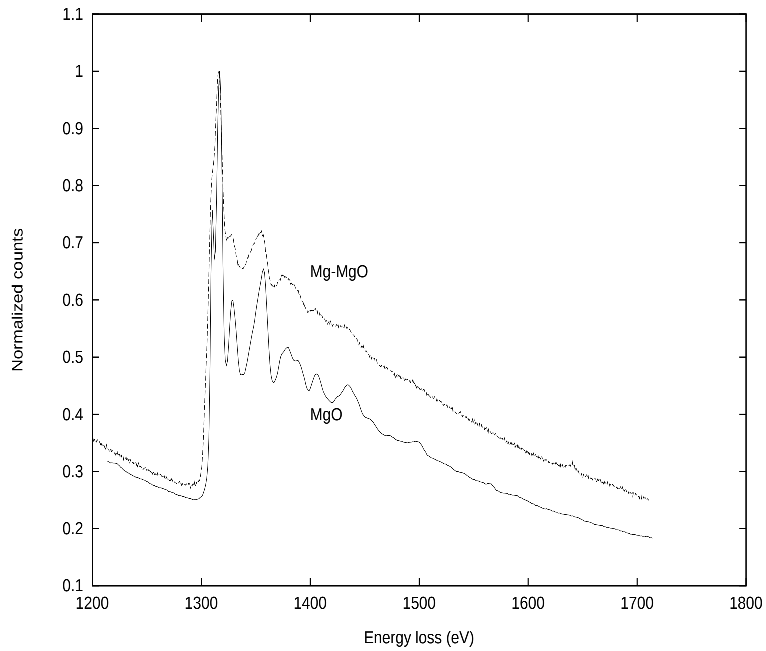

FIG. 8. EELS spectra displaying Mg K-edges, normalized to 1, from the mixed sample and from the pure MgO.

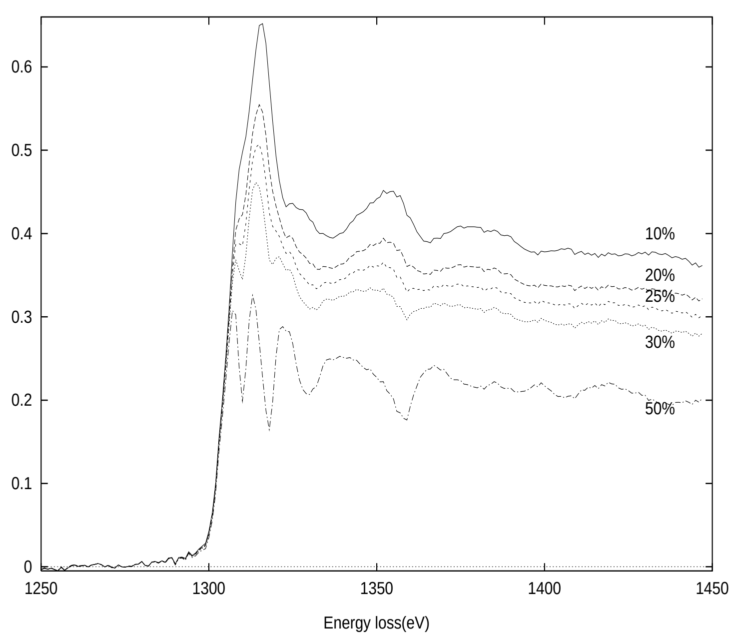

FIG. 9. Different Mg spectra obtained by subtracting varying percentages of pure MgO signal from the total signal. The spectrum obtained after subtracting $\approx 25\%$ is in reasonable agreement with Mg metal data reported in [27]. This percentage is consistent with the results found in the fitting.

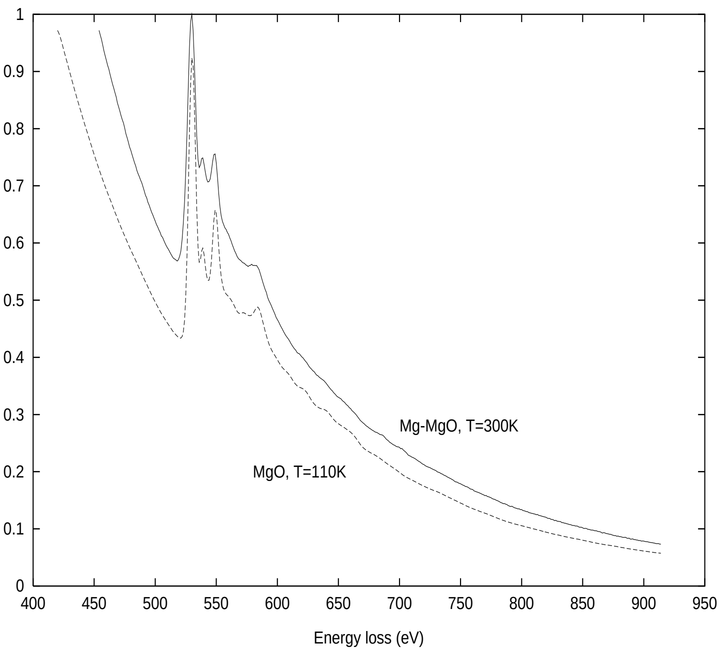

FIG. 10. EELS spectra displaying O K-edge obtained from the MgO/Mg sample superimposed to that obtained in pure MgO at 110K. Since the pure MgO data were taken with a higher resolution, a 1 eV broadening was applied to the data by convoluting with a gaussian. The same ELNES features are observed in both spectra.